

Supplemental information

Glutamate in primary afferents

is required for itch transmission

Lian Cui, Jeff Guo, Suna L. Cranfill, Mayank Gautam, Janardhan Bhattarai, William Olson, Katherine Beattie, Rosemary C. Challis, Qinxue Wu, Xue Song, Tobias Raabe, Viviana Gradinaru, Minghong Ma, Qin Liu, and Wenqin Luo

Supplemental Information – Table of Contents

1. Supplemental Tables

Table S1, related to Figure 1: Summary of peripheral light-evoked behavioral response percentages in six-month-old *Mrgpra3*^{Cre}; *Rosa*^{ChR2ff} mice.

Table S2, related to Figure 2: Summary of pruritogen-evoked scratch bouts over 30 minutes following chemical injection in juvenile *Mrgpra3-Vglut2* CKO mice.

Table S3, related to STAR Methods: RT-PCR primers.

2. Supplemental Figures

Figure S1, related to Figure 1: ChR2 expression in the DRG and spinal cord of *Mrgpra3-ChR2* mice, and characterization of itch-related behaviors.

Figure S2, related to Figure 1: Monosynaptic and polysynaptic inputs to spinal cord dorsal horn neurons from MRGPR $A3^+$ afferents, and light-evoked behavioral responses in *Mrgpra3-ChR2* mice.

Figure S3, related to Figure 2: MRGPR $A3^+$ afferent-specific *Vglut2* CKO mice.

Figure S4, related to Figure 2: Young *Mrgpra3-Vglut2* CKO mice display bafilomycin A1-dependent synaptic vesicle release and show normal somatosensory behaviors.

Figure S5, related to Figure 4: *Mrgpra3-Vglut2* CKO mice display normal behaviors in mechanical threshold or thermosensation tests at six months or older.

Figure S6, related to Figure 5: Molecular characterization of NMBR $^+$ cells in the superficial layer of the spinal cord dorsal horn.

Figure S7, related to Figure 7: Generation of *Mrgpra3-Nmb* CKO mice.

3. Supplemental Figure Legends

1. Supplemental Tables

Table S1. Summary of peripheral light-evoked behavioral response percentages in six-month-old *Mrgpra3^{Cre}; Rosa^{ChR2f/f}* mice, related to Figure 1.

	5 mW	10 mW	20 mW	25 mW
Cheek				
Scratching (S)	0.0 ± 0.0%	4.0 ± 8.9%	4.0 ± 8.9%	0.0 ± 0.0%
Hind paw lifting (PL)	16.0 ± 8.9%	8.0 ± 11.0%	32.0 ± 22.8%	24.0 ± 16.7%
Head shaking (HS)	8.0 ± 11.0%	28.0 ± 22.8%	76.0 ± 35.8%	76.0 ± 8.9%
Bilateral wiping (BW)	40.0 ± 20.0%	84.0 ± 21.9%	96.0 ± 8.9%	96.0 ± 3.9%
Unilateral wiping (UW)	0.0 ± 0.0%	0.0 ± 0.0%	4.0 ± 8.9%	0.0 ± 0.0%
Nape				
Scratching (S)	52.0 ± 22.8%	64.0 ± 16.7%	60.0 ± 24.5%	64.0 ± 43.4%
Hind paw lifting (PL)	8.0 ± 17.9%	12.0 ± 17.9%	16.0 ± 16.7%	0.0 ± 0.0%
Head shaking (HS)	96.0 ± 8.9%	100 ± 0.0%	96.0 ± 8.9%	96.0 ± 8.9%
Bilateral wiping (BW)	4.0 ± 8.9%	20.0 ± 34.6%	16.0 ± 16.7%	36.0 ± 32.9%
Unilateral wiping (UW)	8.0 ± 11.0%	4.0 ± 8.9%	24.0 ± 26.1%	24.0 ± 21.9%

Table S2. Summary of pruritogen-evoked scratch bouts over 30 minutes following chemical injection in juvenile *Mrgpra3-Vglut2* CKO mice, related to Figure 2.

Numbers in parenthesis are the sample size of each cohort.

	<i>Mrgpra3-Vglut2</i> CKO		Control	
	Cheek	Nape	Cheek	Nape
Chloroquine (CQ)	158.8 ± 25.3 (12)	293.1 ± 35.4 (7)	92.3 ± 17.2 (9)	329.8 ± 36.1 (4)
Histamine	57.3 ± 6.8 (6)	n/a	46.4 ± 9.0 (8)	n/a
BAM8-22	48.0 ± 13.8 (6)	41.9 ± 8.6 (11)	42.0 ± 16.1 (5)	39.7 ± 7.0 (12)
SLIGRL	54.4 ± 8.2 (7)	178.8 ± 35.7 (8)	47.2 ± 5.1 (9)	114.7 ± 19.6 (9)
5-HT	97.8 ± 19.2 (5)	n/a	86.6 ± 11.6 (9)	n/a

Table S3. RT-PCR primers, related to STAR Methods.

Gene	Primer 1	Primer 2
<i>Vglut1</i>	5'-GCAGGAGGGAGTTCGGAAG-3'	5'-ACAATGGCAAAGCCAAGAC-3'
<i>Vglut2 (pair 1)</i>	5'-GGAGAAGAACAGCAGGACAACC-3'	5'-TAGCCCCAGAAGAACGATCC-3'
<i>Vglut2 (pair 2)</i>	5'-GGGGAAAGAGGGGATAAAGA-3'	5'-CTGCAGATGGATCAGCATA-3'
<i>Vglut3</i>	5'-TGTGTCATGGGTGTGAGGAT-3'	5'-TGATGGCATAGACAGGCAAG-3'
<i>Grp</i>	5'-TCCTGGCTAACGATGTATCCG-3'	5'-AGTCTACCAACTTAGCGGTTG-3'
<i>Grpr</i>	5'-ACTGTCAGCTGACAGGTACAAAG-3'	5'-TAGGCACTCTGAATCAGATTTC-3'
<i>Nmbr</i>	5'-CAACCTCTCCTTCCCACAG-3'	5'-GTCCATGGGGITTCACGATAG-3'
<i>Gapdh</i>	5'-GGTGAAGGTCGGTGTGAACG-3'	5'-CTCGCTCCTGGAAGATGGT-3'

2. Supplemental Figures

Figure S1

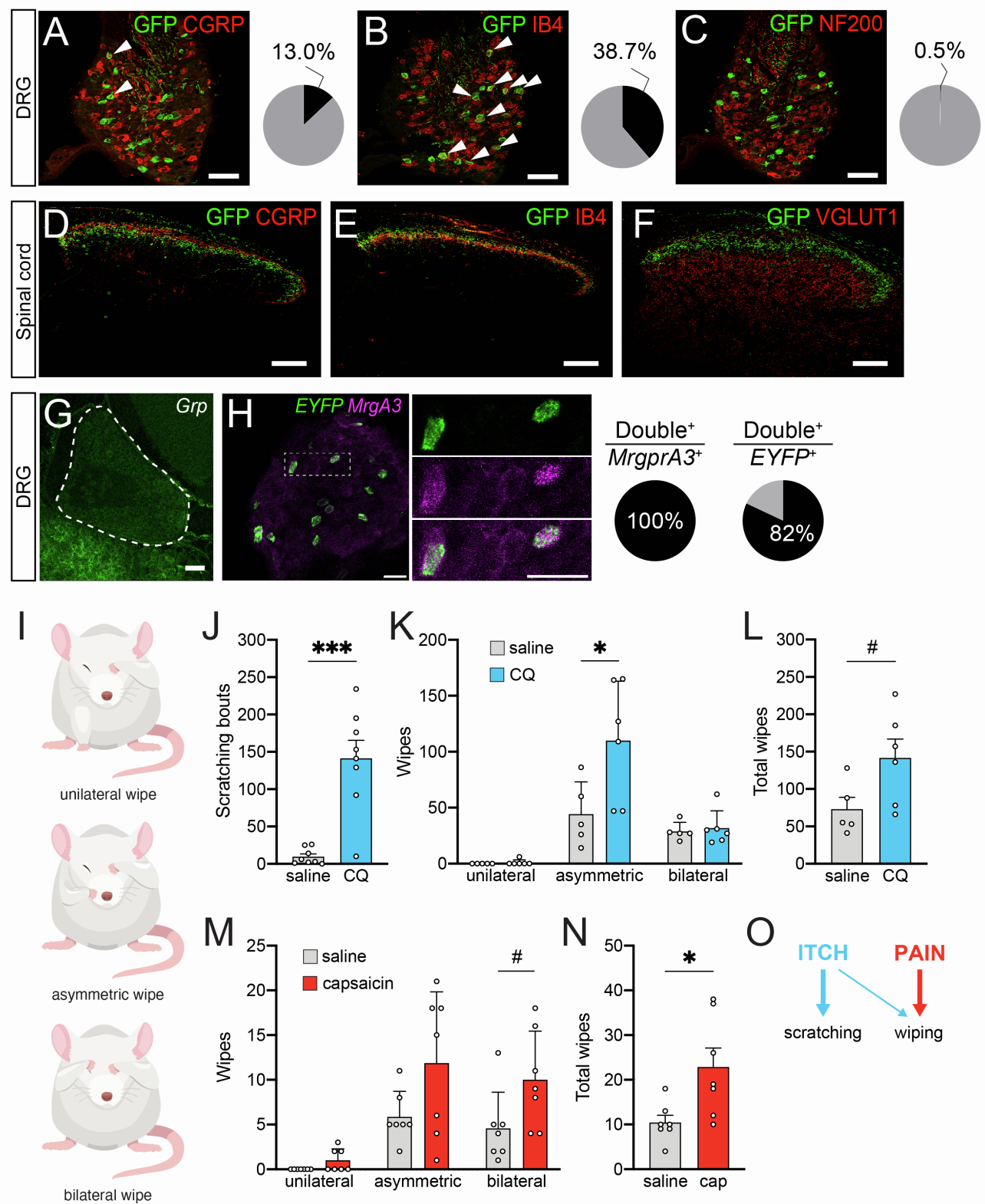


Figure S2

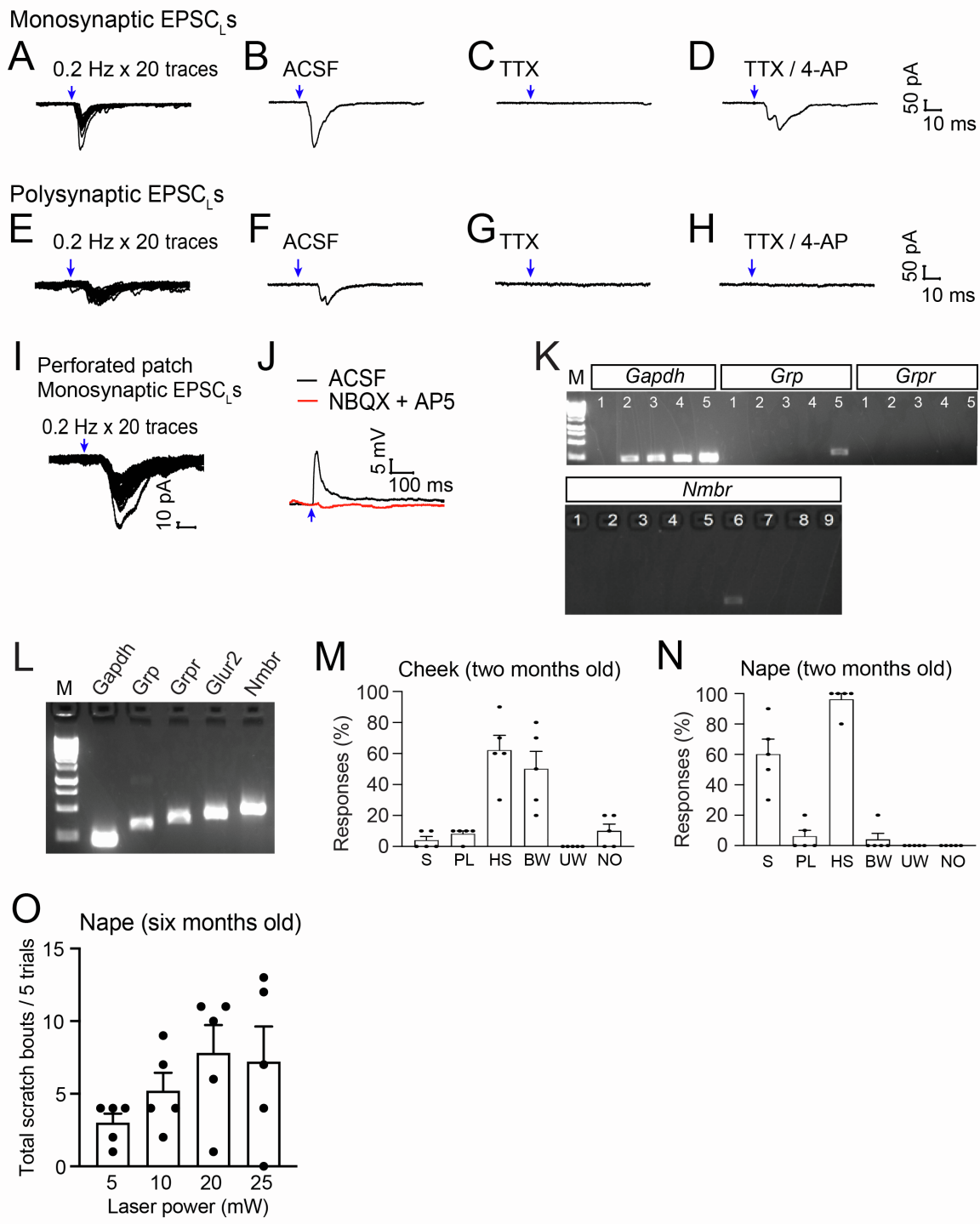
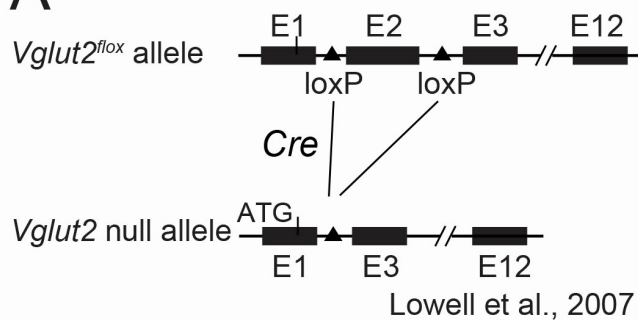
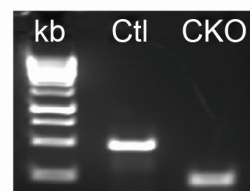


Figure S3

A



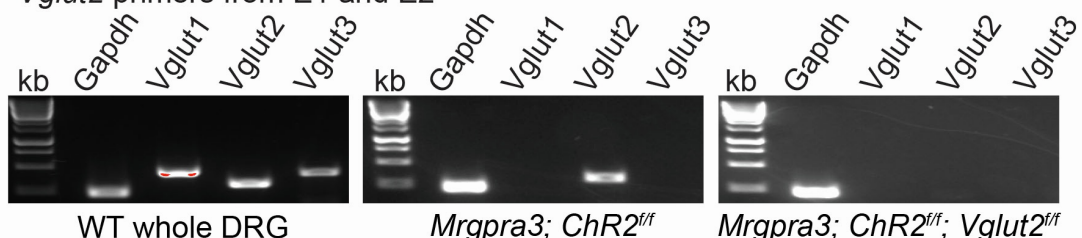
B *Vglut2* primers from E1 and E3



Control: Whole protein (582aa)
CKO: Truncated protein (66aa)
MESVKQRILAPGKEGIKNFAGKPLGQIYRKPNL
TGTPRPWGDPRIVLLGLYHHPDSRRIYRIAAGC

C

Vglut2 primers from E1 and E2



Vglut2
Mrgpra3
Vglut2

Mrgpra3
Vglut1
Vglut2
Vglut3

Overlay
Gapdh
Vglut1
Vglut2
Vglut3

Gapdh
Vglut1
Vglut2
Vglut3

Mrgpra3
Vglut2
Vglut2

Mrgpra3
Vglut1
Vglut2
Vglut3

Overlay
Gapdh
Vglut1
Vglut2
Vglut3

Gapdh
Vglut1
Vglut2
Vglut3

Mrgpra3
Vglut2
Vglut2

Mrgpra3
Vglut1
Vglut2
Vglut3

Overlay
Gapdh
Vglut1
Vglut2
Vglut3

Gapdh
Vglut1
Vglut2
Vglut3

Figure S4

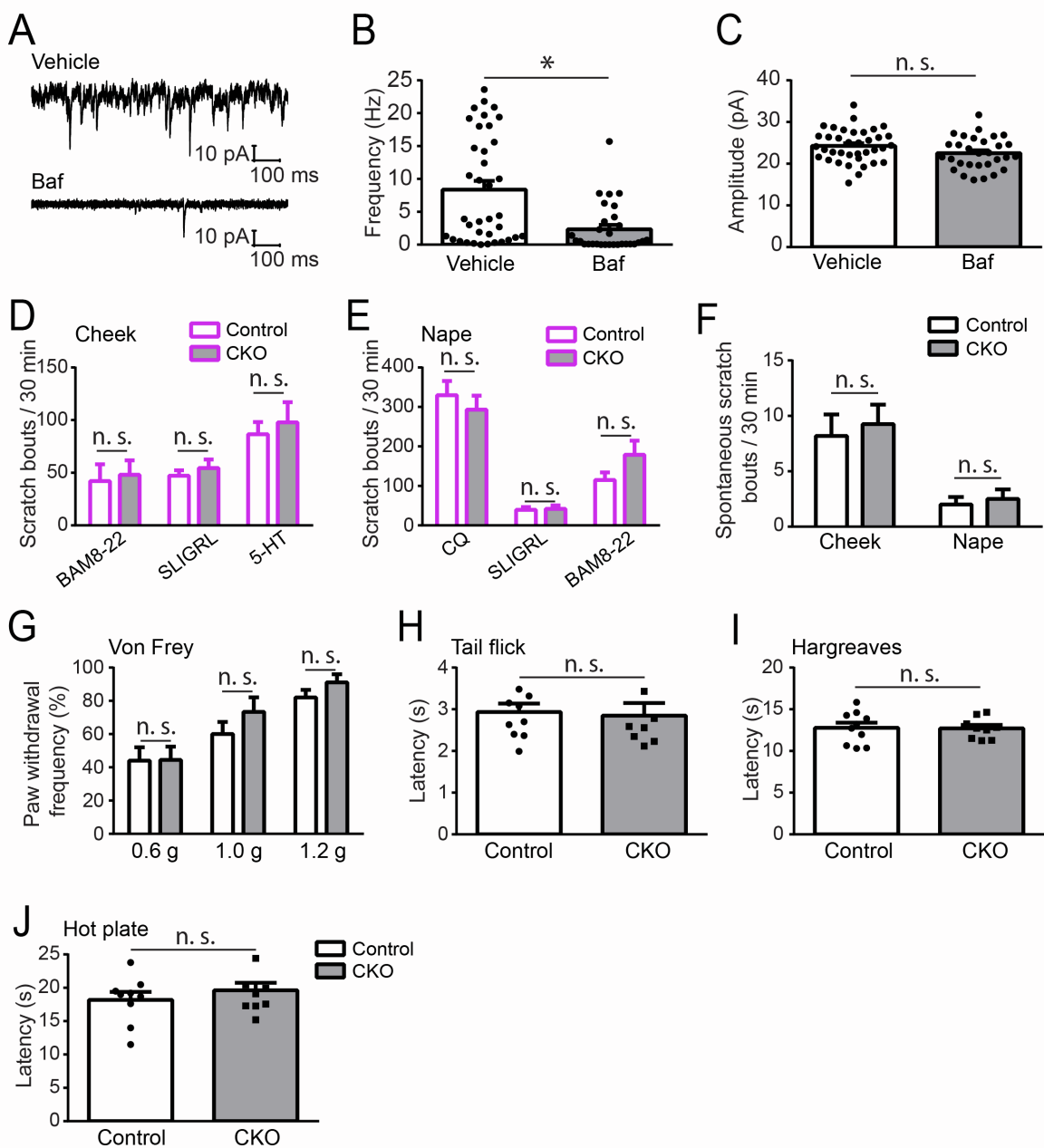


Figure S5

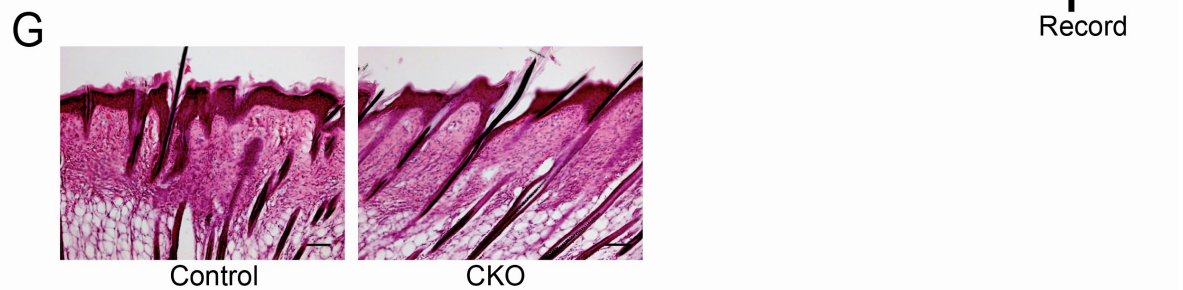
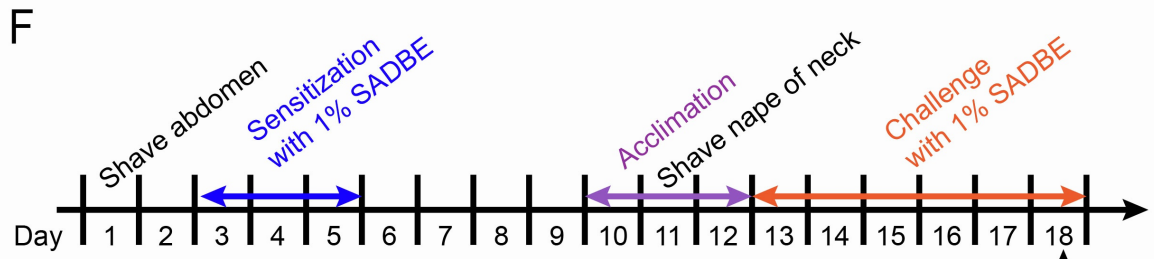
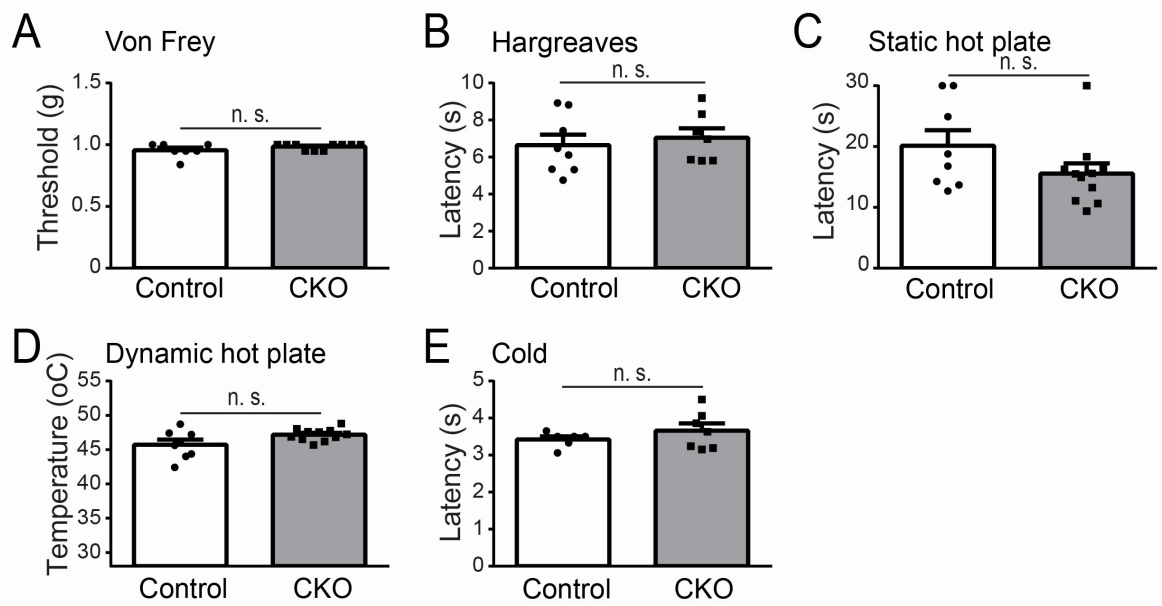


Figure S6

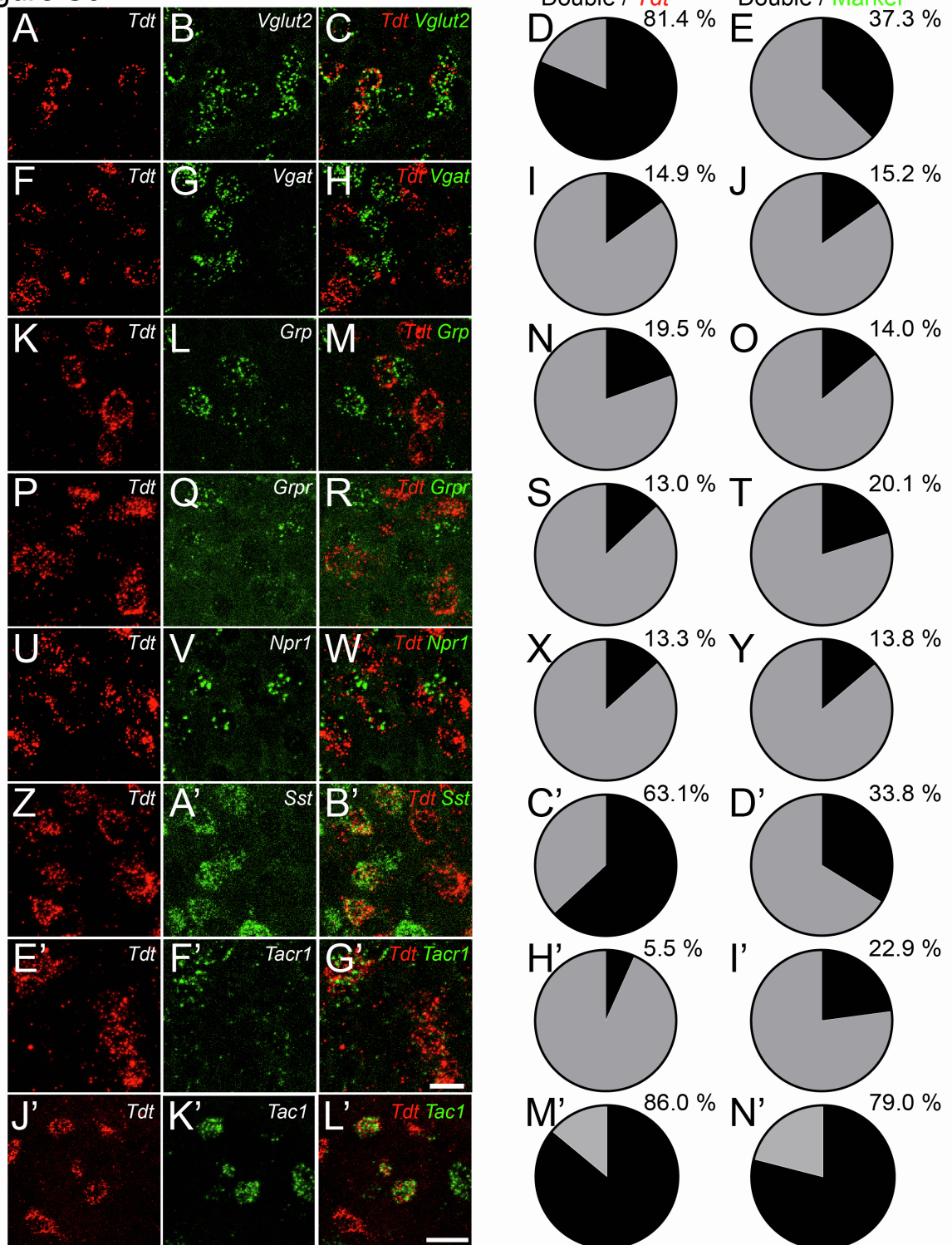
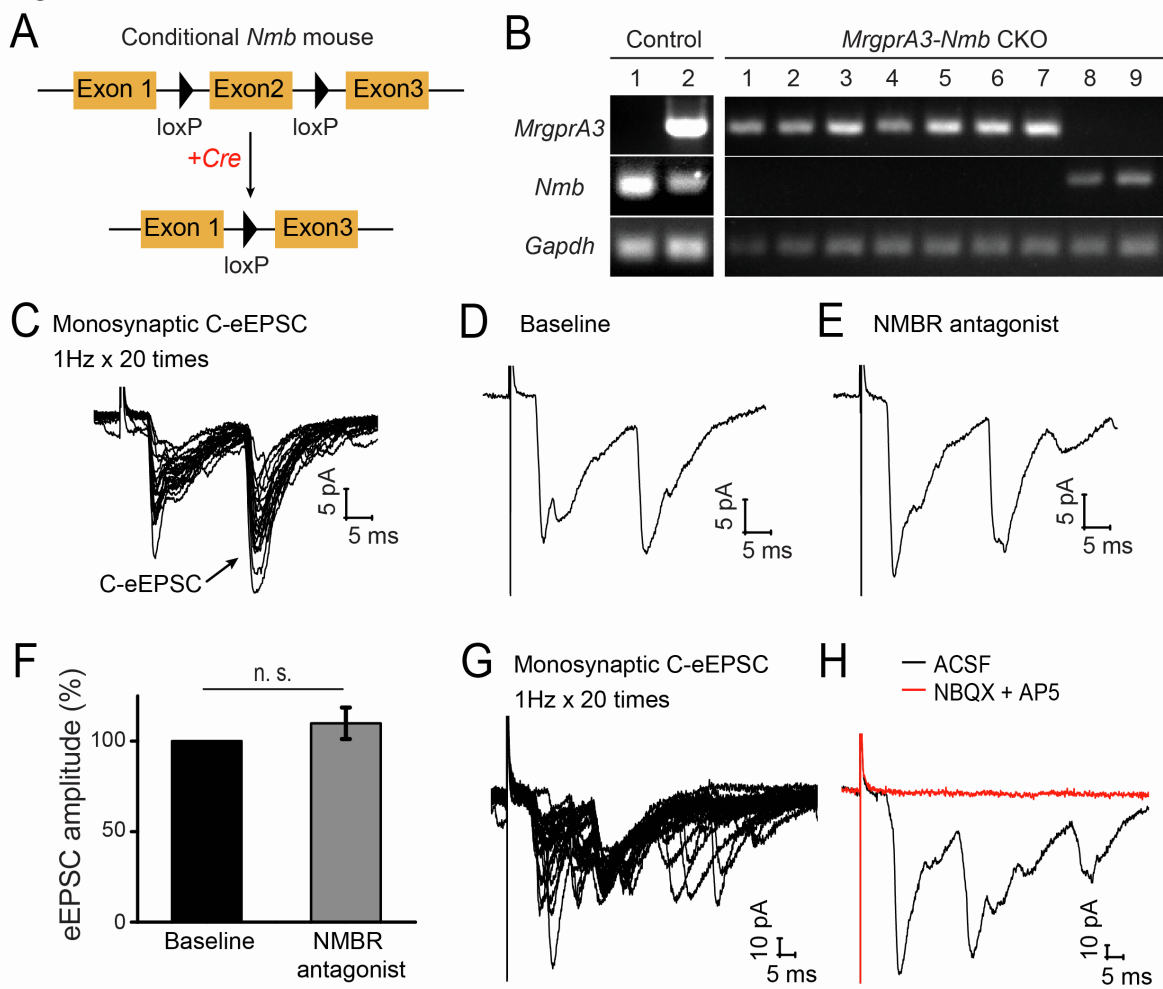


Figure S7



3. Supplemental Figure Legends

Supplemental Figure 1. ChR2 expression in DRG and spinal cord of *Mrgpra3-ChR2* mice, and characterization of itch-related behavior, related to Figure 1.

(A-C) Double immunostaining of ChR2-EYFP and CGRP (A), ChR2-EYFP and IB4 (B), and ChR2-EYFP and NF200 (C) with lumbar (L4 and L5) DRG sections of three-week-old *Mrgpra3-ChR2* mice. Pie charts show the percentage of ChR2-EYFP⁺ DRG neurons that are double-positive for the indicated marker. Scale bars: 50 μm. 6-8 sections/mouse, n=3. (D-F). Double immunostaining of ChR2-EYFP and CGRP (D), ChR2-EYFP and IB4 (E), and ChR2-EYFP and VGLUT1 (F) with lumbar spinal cord sections of three-week-old *Mrgpra3-ChR2* mice. Scale bars: 50 μm. 6-8 sections/mouse, n=3. (G) RNAscope *in situ* hybridization of *Grp* with lumbar (L4 and L5) DRG sections of three-week-old wild type mice. Scale bar: 50 μm. 6-8 sections/mouse, n=3. (H) Double RNAscope *in situ* hybridization of *EYFP* and *MrgprA3* with lumbar DRG sections of six-week-old *Mrgpra3-ChR2* mice. Dashed outline indicates inset, magnified to the right. Scale bars: 50 μm. 6-8 sections/mouse, n=3. (I) Illustration of unilateral wiping (contralateral forepaw on the ground), asymmetric wiping, and bilateral (symmetric) wiping. (J) Total scratching bouts over 30 minutes in response to chloroquine (20 mM) or saline cheek intradermal injections in C57BL/6J mice. (K-N). Wiping responses to chloroquine or saline cheek injections (K and L) and capsaicin eye drops (0.06 μg/μl, 90 seconds) (M and N) in C57BL/6J mice. Each dot represents a single mouse. Data is presented as mean ± SD. Welch's t test in J, L, and N; unpaired student's t test in K and M. *p<0.05; ***p<0.0001, #p=0.0557, n=5-8. (O) Schematic of how scratching and wiping may perform as behavioral readouts of itch and pain sensations.

Supplemental Figure 2. Monosynaptic and polysynaptic inputs to spinal cord dorsal horn neurons from MRGPR $A3^+$ afferents, and light-evoked behavioral responses in *Mrgpra3-ChR2* mice, related to Figure 1.

(A-D) Representative traces of monosynaptic EPSC_{LS}s recorded from dorsal horn neurons using spinal cord slices of 4-6w *Mrgpra3-ChR2* mice. Superimposition of monosynaptic EPSC_{LS}s induced by 20 times light stimuli at 0.2 Hz (A). Baseline EPSC_{LS} (B) was blocked by TTX (1 μ M) treatment (C), but recovered by perfusion of TTX (1 μ M) and 4-AP (4 mM) (D). (E-H) Representative traces of polysynaptic EPSC_{LS}s recorded from dorsal horn neurons. Superimposition of polysynaptic EPSC_{LS}s induced by 20 times light stimuli at 0.2 Hz (E). Baseline EPSC_{LS} (F) was blocked by TTX (1 μ M) treatment (G), but not recovered by perfusion of TTX (1 μ M) and 4-AP (4 mM) (H). The blue arrows indicate laser stimuli. (I and J) In perforated patch recordings of superficial DH neurons from spinal cord slices of four- to six-week-old *Mrgpra3-ChR2* mice using amphotericin B (100 μ g/mL), light stimulation-induced monosynaptic responses (black trace) were blocked by glutamate receptor antagonists (red trace). (K) RT-PCR of *Gapdh*, *Grp*, *Grpr*, *Glur2*, and *Nmbr* with RNAs from the whole spinal cord of wild type mice. (L) Single cell RT-PCR of *Gapdh*, *Grp*, *Grpr*, and *Nmbr* of monosynaptic responsive spinal DH neurons in spinal cord slices by light stimulation in five- to six-week-old *Mrgpra3-ChR2* mice. (M and N) The percentage of behavioral responses to 20 mW blue laser stimulation of the cheek (M) or nape (N) of two-month-old *Mrgpra3-ChR2* mice. Cheek: scratching (S) $4.0 \pm 2.5\%$, hind paw lifting (PL) $8.0 \pm 2.0\%$, head shaking (HS) $62.0 \pm 9.7\%$, bilateral wiping (BW) $50.0 \pm 11.4\%$, unilateral wiping (UW) $0.0 \pm 0.0\%$. Nape: scratching (S) $60.0 \pm 10.0\%$, hind paw lifting (PL) $6.0 \pm 4.0\%$, head shaking (HS) $96.0 \pm 4.0\%$, bilateral wiping (BW) $4.0 \pm 4.0\%$, unilateral wiping (UW) $8.0 \pm 11.0\%$. (O) Total scratch bouts over 5 trials of peripheral blue laser stimulation at the nape of six-month-old *Mrgpra3-ChR2* mice, as in Fig. 1C. Each dot represents an individual mouse.

Supplemental Figure 3. MRGPR $A3^+$ afferent-specific *Vglut2* CKO mice, related to Figure 2.

(A) Genomic structure of conditional *Vglut2* allele and *Vglut2* null allele after Cre mediated recombination.

(B) Single cell RT-PCR of *Vglut2* (PCR primers in exons 1 and 3) with dissociated EYFP $^+$ DRG neurons from three- to four-week-old *Mrgpra3-ChR2* (control) and *Mrgpra3-Vglut2* (CKO) mice. The PCR products were sequenced, and the protein sequence predicted from the *Vglut2* null DRG neuron is shown. Control: 6 neurons/mice from 3 mice; CKO: 6 neurons/mice from 3 mice. (C) RT-PCR of *Gadph*, *Vglut1*, *Vglut2*, and *Vglut3* using RNA extracts from a whole DRG of a WT mouse (left) and dissociated single examples of EYFP $^+$ DRG neurons of control (middle) and CKO (right) mice. Control: 14 neurons from 2 mice; CKO: 14 neurons from 2 mice. (D-G) Double fluorescent *in situ* hybridization of *Mrgpra3* (green) and transcripts of *Vglut1* or *Vglut3* (red) with DRG sections of three-week-old *Vglut2^{ff}* (control) and *Mrgpra3-Vglut2* (CKO) mice. Images in the rectangles are enlarged. White dashed circles indicate *Vglut1⁺* or *Vglut3⁺* but *Mrgpra3⁻* neurons. Yellow dashed circles indicate *Mrgpra3* expressing neurons. Scale bars, 50 μ m. 6-8 sections/mouse, n=3 mice.

Supplemental Figure 4. Juvenile *Mrgpra3*-*Vglut2* CKO mice display bafilomycin A1-dependent synaptic vesicle release and show normal somatosensory behaviors, related to Figure 2.

(A) Representative traces of sEPSCs after vehicle (0.1% DMSO) or bafilomycin A1 (4 mM) treatment of spinal cord slices of four- to six-week-old CKO mice. (B and C) Quantification of frequency and amplitude of sEPSCs under different conditions. (D) Quantification of scratching induced by cheek injections of BAM8-22, SLIGRL, and 5-HT in control and CKO mice that are around two months old. (E) Quantification of scratching in response to nape injection of CQ, SLIGRL, and BAM8-22 in control and CKO mice. (F) Quantification of spontaneous scratching of *Vglut2*^{ff} (control) and *Mrgpra3*^{Cre}; *Vglut2*^{ff} (CKO) mice that are around two months old. (G) Paw withdrawal frequency of control and CKO mice in responses to different Von Frey hairs around two months old. 0.6g: control $44.0 \pm 8.0\%$ vs CKO $44.4 \pm 8.0\%$, p>0.05; 1.0g: control $60.0 \pm 7.3\%$ vs CKO $73.3 \pm 8.8\%$, p>0.05; 1.2g: control $82.0 \pm 4.7\%$ vs CKO $91.1 \pm 4.8\%$, p>0.05. (H) Tail withdrawal latency of control and CKO mice in tail flick test. Control 2.9 ± 0.2 s vs CKO 2.8 ± 0.3 s, p>0.05. (J and K) Paw withdrawal latency of control and CKO mice in Hargreaves test and hot plate test. Hargreaves test: control 12.8 ± 0.6 s vs CKO 12.7 ± 0.4 s, p>0.05. Hot plate test: control 18.2 ± 1.2 s vs CKO 19.6 ± 1.1 s p>0.05. For the mechanical and thermal sensitivity assays: control n=9-10, CKO n=8-9. Data is presented as mean \pm SEM. Unpaired student's t-test in B-J, * p<0.05; n.s., not significant.

Supplemental Figure 5. *Mrgpra3-Vglut2* CKO mice display normal behaviors in mechanical threshold or thermosensation tests at six months or older, related to Figure 4.

(A) Paw withdrawal threshold in Von Frey test in six-month-old or older control and CKO mice. Control 0.96 ± 0.02 g, n=7 vs CKO 0.99 ± 0.01 g, n=10, p>0.05. (B and C) Paw withdrawal latency in the Hargreaves test and static hot plate test in control and CKO mice. Hargreaves test: control 6.65 ± 0.57 s, n=8 vs CKO 7.05 ± 0.51 s, n=7, p>0.05. Static hot plate test: control 20.14 ± 2.54 s, n=8 vs CKO 15.57 ± 1.67 s, n=11, p>0.05. (D) Paw withdrawal threshold in the dynamic hot plate test in control and CKO mice. Control 45.72 ± 0.73 °C, n=8 vs CKO 47.19 ± 0.27 °C, n=11, p>0.05. (E) Paw withdrawal latency in the cold sensation test in control and CKO mice. Control 3.42 ± 0.08 , n=6 vs CKO 3.66 ± 0.19 , n=7, p>0.05. (F) Timeline for generating the SADBE-induced ACD mouse model. (G) H&E staining of the nape skin in control and CKO mice after SADBE treatment. Scale bars: 100 μm. Data is presented as mean ± SEM. Unpaired student's t-test in A-E, n.s., not significant.

Supplemental Figure 6. Molecular characterization of NMBR⁺ cells in the superficial layer of the spinal cord dorsal horn, related to Figure 5.

(A-N') RNAscope *in situ* hybridizations of *Tdt* and *Vglut2*, *Vgat*, *Grp*, *Grpr*, *Npr1*, *Sst*, *Tacr1*, and *Tac1* in lumbar spinal cord sections of three-week-old *Nmbr-Tdt* mice. Scale bars: 10 μm. Pie charts summarize the quantification of double-positive cells among *Tdt*⁺ cells or marker⁺ cells. 6-8 sections/mouse, n=3 mice.

Supplemental Figure 7. Generation of *Mrgpra3-Nmb* CKO mice, related to Figure 7.

(A) Illustration of the genomic structure of the conditional *Nmb* allele and Cre-dependent recombination. (B) Single cell RT-PCR of *Mrgpra3*, *Nmb*, and *Gapdh* in dissociated DRG neurons from *Nmb^{ff}* (control) and *Mrgpra3-Nmb* (CKO) mice. Control n=3 mice; CKO n=3 mice. (C) Representative traces of monosynaptic EPSCs (C-eEPSCs) recorded in *Nmbr-Tdt* neurons after dorsal root electrical stimulation (C afferent stimulation). (D and E) Representative paired C-eEPSC traces at baseline (D) and after perfusion of the NMBR antagonist BIM 23042 (6 μM) (E). (F) Quantification of C-eEPSC amplitude, n=4. (G and H) Monosynaptic C-eEPSCs were blocked by glutamate receptor antagonists, NBQX (20 μM) and AP5 (50 μM) (red traces).